ARTICLES

Stochastic Cellular Automata Models of Molecular Excited-State Dynamics

Paul G. Seybold*

Departments of Chemistry and Biochemistry, Wright State University, Dayton, Ohio 45435

Lemont B. Kier*

Department of Medicinal Chemistry, Virginia Commonwealth University, Richmond, Virginia 23298

Chao-Kun Cheng

Department of Mathematical Sciences, Virginia Commonwealth University, Richmond, Virginia 23298

Received: September 12, 1997

A probabilistic asynchronous cellular automaton described previously [Seybold, Kier, and Cheng, *J. Chem. Info. Comput. Sci.* **1997**, *37*, 386−391] has been applied to the description of molecular excited-state dynamics. The model simulates in a visual, time-dependent fashion the variations in ground- and excited-state populations that occur under stipulated probabilistic transition rules. Both pulse mode and steady-state conditions can be simulated. The deterministic values for the fluorescence lifetime (τ_f), the phosphorescence lifetime (τ_p), and the quantum yields of fluorescence (ϕ_f), triplet state formation (ϕ_T), and phosphoresence (ϕ_p) arise as limiting cases for large numbers of cells or large numbers of trials. Since each trial is an independent "experiment", stochastic variations in the populations and properties can be estimated from repeated trials. Phenomena such as ground-state depletion and population inversion under high radiation intensity arise naturally within the model.

Introduction

Spectroscopy is the main avenue through which the details of molecular dynamics and structure are approached. In particular, spectroscopic studies of excited molecular electronic states over the years have provided a rich store of information about the behavior of these important species. Technological advances during the past several decades have permitted more and more sensitive detection of smaller samples, to the point that at the present time studies of single molecules are increasingly reported.[1−9] The traditional approach to the analysis of molecular excited-state dynamics relies on sets of coupled differential equations that describe the macroscopic behavior of the examined system in the limit of large sample size. This approach is obviously not well-suited to the analysis of small samples, nor does it provide information on the stochastic aspects of the dynamics or capture well the inherently dynamic natures of the processes involved.

Cellular automata, although not presently widely applied in chemistry, offer a very different and potentially highly insightful approach to the analysis of the dynamical behavior of molecular systems. We have recently described a probabilistic cellular automaton capable of accurately simulating processes of first-order chemical kinetics.[10] The cellular automaton simulates, for example, the stochastic behaviors expected in exponential decay, consecutive reactions, first-order equilibria, rate-limiting steps, pre-equilibria, and other classic processes in chemical kinetics. The deterministic solutions, as given by the traditional macroscopic analysis, emerge as limiting cases of the cellular automata approach. In this report we describe application of this cellular automata approach to the general treatment of molecular excited-state behavior. In later reports we will describe applications of the model to specific molecular species and also to such phenomena as laser action, luminescence quenching, and energy transfer.

The Traditional Approach

Studies of molecular excited-state dynamics are typically carried out in one of two modes: *pulse* mode and *steady-state* mode. In the pulse mode a flash (often from a laser) excites the system, and the subsequent evolution of the system is monitored by observing the time course of emission or absorption processes.[11] Typically this mode provides information about such details of the dynamics as the fluorescence and phosphorescence lifetimes, triplet−triplet absorption spectra, the appearance and decay rates of intermediates, and possibly events related to energy transfer and other time-dependent processes. In the steady-state mode excitation is continuous. This mode is normally employed to find the luminescence spectra and, using any of a variety of techniques, the quantum yields of fluorescence, phosphorescence, and triplet formation.

Within this framework the excited-state dynamics of a molecule are understood by determining the rate constants of its radiative and nonradiative excited-state transitions.[12,13] In the simplest and most typical case the dynamics of organic molecules can be interpreted in terms of just three states: the

S1089-5639(97)02985-X CCC: $15.00
Published on Web 01/16/1998

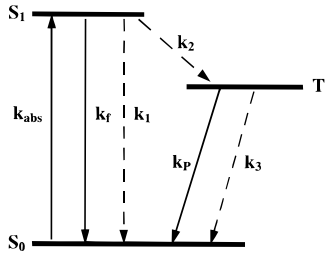

Figure 1. Jablonski diagram of molecular electronic states: radiative transitions are indicated by solid lines and nonradiative transitions by dashed lines.

ground state S_0, the lowest excited singlet state S_1, and the lowest triplet state T. The relationship of these states is illustrated by a Jablonski diagram,[14−16] as shown in Figure 1. As first noted by Kasha, because of the rapidity of intramolecular nonradiative conversions among higher excited states, most organic molecules emit significant luminescence only from their lowest excited states of a given multiplicity: fluorescence from the lowest excited singlet state and phosphorescence from the lowest triplet state.[17] Exceptions to this rule, such as azulene, are naturally of special interest, and the diagram can be modified accordingly.

The excited-state dynamics are governed by the coupled differential rate equations that describe the production and depletion of the ground and excited states.[14,15] In the above simple case these rate equations are

$$\frac{d[S_0]}{dt} = -k_{abs}[S_0] + (k_f + k_1)[S_1] + (k_p + k_3)[T] \quad (1)$$

$$\frac{d[S_1]}{dt} = k_{abs}[S_0] - (k_f + k_1 + k_2)[S_1] \quad (2)$$

$$\frac{d[T]}{dt} = k_2[S_1] - (k_p + k_3)[T] \quad (3)$$

Here k_{abs} represents a product of the Einstein coefficient of stimulated absorption B_{mn} and the radiation field intensity $\rho(\nu)$ at the frequency ν of the exciting radiation, as modified by experimental conditions according to Beer's law. Equations 1−3 lead to the following expressions for the fluorescence lifetime (τ_f), the phosphorescence lifetime (τ_p), and the quantum yields of fluorescence (ϕ_f), triplet state formation (ϕ_T), and phosphoresence (ϕ_p) in terms of the rate constants:

$$\tau_f = 1/(k_f + k_1 + k_2)$$

$$\tau_p = 1/(k_p + k_3)$$

$$\phi_f = k_f/(k_f + k_1 + k_2)$$

$$\phi_T = k_2/(k_f + k_1 + k_2)$$

$$\phi_p = k_p\phi_T/(k_p + k_3)$$

The fluorescence *natural radiative lifetime*, defined as $\tau_{nr} = 1/k_f$, is the lifetime of the excited singlet state expected if competing nonradiative decay modes were absent; experimentally it can be estimated from the absorption spectrum.

Equations 1−3 are deterministic in the sense that they represent absolute behaviors expected in the limit of very large numbers of molecules. These equations provide no information on the stochastic fluctuations expected in the values of the properties described, nor are they expected to be reliable descriptions of behavior as the limit of small numbers of molecules is approached.

Cellular Automata

Cellular automata were first proposed by Ulam[18] and von Neuman[19] a half century ago, but only with the more recent development of modern digital computers has their scientific potential begun to be fully realized. In their most common form cellular automata consist of a rectangular grid composed of cells, in which each cell can exist in a number of discrete states. Given a specific starting configuration of the cells, evolution of the system is governed by a set of local rules. These rules are applied at every time iteration of the automaton, so that cellular automata, unlike the conventional approach, are discrete not only in state but also in space and time. The rules are normally of two types: *movement* rules, which determine whether a cell will move to an adjacent space on the grid, and state *transition* rules, which determine if a cell will change its state, and can be either fixed or probabilistic in nature. Evolution of a particular system according to its local rules frequently leads to the appearance of unexpected patterns, called *emergent properties*, which in many important cases can be associated with related natural phenomena. Because of the almost unlimited possibilities for the rules and starting conditions, the simple cellular automaton concept leads to an enormous variety of possible realizations, and cellular automata have been applied to a wide range of applications in both physics[20−25] and biology,[26−28] and to a lesser extent in social science[29] and chemistry.[30−32]

Kier and Cheng have recently developed a series of computer programs utilizing asychronous probabilistic cellular automata. In these, an $n \times m$ grid of cells evolves in a series of time-step iterations according to probabilistic rules; the procedure is asynchronous in the sense that at each iteration each cell, in random order, is given a chance to move and/or change its state. The possible states are conveniently represented by different cell colors. Applications have included water structure,[33] solution phenomena,[34−36] partitioning of a solute between two liquids,[37] micelle behavior,[35,38] diffusion,[39] enzyme kinetics,[40] and membrane permeability.[41]

Application to Excited-State Dynamics

As noted, we recently presented a cellular automaton model for first-order kinetics and demonstrated its application to a number of classic examples of first-order chemical kinetics processes.[10] The first-order kinetics cellular automaton realization is especially simple since only state transition rules are needed, and these rules are independent of the cells' surroundings. Because the state transition rules are probabilistic, each "run" of the system is an independent trial, potentially leading to a different result. However, in the limit of a large number of cells (i.e., grid size $n \times m = N$) in the system, the overall behavior approaches that expected from the traditional deterministic model. By using multiple runs, the stochastic behavior, as well as the average behavior, of the system can be determined. Further details are found in our previous study.[10]

We have developed two models for the simulation of molecular excited-state dynamics, as shown in Figure 2. In the most simple model (Figure 2a) only three states (A, B, and C) are included, and probabilities P_{ij} for transitions between these states are assigned to represent in a relative manner the total transition probabilities expected between the corresponding states of Figure 1. Although this simple model does not distinguish competing radiative and nonradiative transitions, it

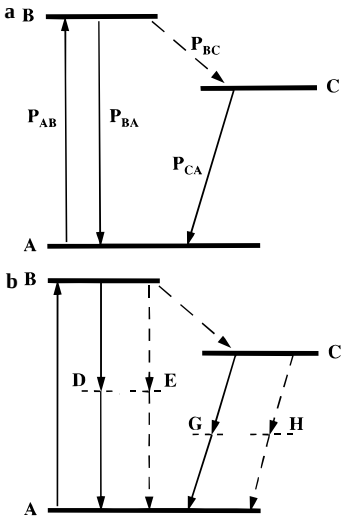

Figure 2. State diagrams for the simple (a) and extended (b) cellular automaton models. In b real states are indicated by solid lines and virtual states by dashed lines.

does allow overall dynamic behavior of the system to be examined and analyzed in an especially simple and heuristic manner. To simulate the "pulse" mode of operation, it is most convenient to assign $P_{AB} = 0$ and start with all N cells in state B: evolution of the system then consists in a cascade from B down to A, partly via state C. One can, for example, determine the excited-state lifetimes τ_B and τ_C from an examination of the time-dependent populations of states B and C. In the "steady-state" mode P_{AB} is assigned a nonzero value, and the populations of the states can be monitored as they evolve to their equilibrium values (with inherent stochastic fluctuations).

A more complete model is shown in Figure 2b. In this, as a counting convenience, we introduce "virtual states"; these states have unity probabilities of decaying to lower states and thus last for only a single iteration. If the probabilities of the "real" transitions are relatively small compared to unity, the presence of these virtual states will have no appreciable effect on the time evolution of the system. By counting transitions through the virtual states one can distinguish radiative and nonradiative transitions and determine the quantum yields ϕ_f, ϕ_T, and ϕ_p; neither these yields nor the lifetimes τ_B and τ_C are altered by the presence of the virtual states. The pulse and steady-state modes can thus be performed in the same manner as for the simple model, but additional details are revealed.

Whereas in the traditional approach the *rate constants* k_i are the fundamental parameters governing the evolution of the system, in the cellular automaton approach the *transition probabilities* P_{ij} play this role. It is convenient to use iterations (itn) as the time units in cellular automaton studies: in the present examples an iteration might be imagined to be equivalent to a nanosecond for the purposes of simulating experimentally observed molecular excited-state dynamics. Statistical analyses of the data were carried out using the StatMost software program.[42]

Results and Discussion

Pulse Mode. The pulse condition was simulated by beginning with all cells in state B and allowing the system to evolve under the conditon $P_{AB} = 0$. In a preliminary examination the simple model of Figure 2a was employed with differing cell numbers N. The transition probabilities were assigned the values $P_{BA} = 0.04$, $P_{BC} = 0.06$, and $P_{CA} = 0.01$, as summarized in the state transition probability matrix **P**.

$$\mathbf{P} = \begin{pmatrix} 0 & 0 & 0 \\ 0.04 & 0.06 & 0 \\ 0.01 & 0 & 0 \end{pmatrix}$$

(Note that only "transitions", i.e., state *changes*, are identified in this notation; the probability that a state remains the same is the residual probability.) These probabilities were designed for purposes of illustration to correspond to the limiting deterministic values $\phi_f = 0.40$, $\tau_B = 10$ itn, and $\tau_C = 100$ itn. Half-lives were measured by following the populations of states B and C as they evolve in time; they can be converted to normal lifetimes using the formula $\tau = \tau_{1/2}/(\ln 2)$.

In the first example a single cell was examined over 10 trials, with the results shown in Table 1. It is clear that there is a great deal of scatter for all the properties in this example. Lifetime results for other cell counts are shown in Table 2. The scatter decreases as the cell count increases, and for the 1000- and 10 000-cell trials the average values for the normal lifetimes ($\tau_B = 9.2$ and 9.48 itn, and $\tau_C = 101.4$ and 101.1 itn, respectively) approach those expected in the deterministic limit. Plots of the populations of the B and C states as functions of time are shown in Figure 3; these plots are seen to bear a strong resemblance to the luminescence decay curves typically obtained in photon-counting experiments with dyes.

The seven-state extended model shown in Figure 2b permits a more detailed analysis of the quantum yields and decay pathways. For purposes of illustration the transition probability matrix **P′** was set as follows:

$$\mathbf{P'} = \begin{pmatrix} 0 & 0 & 0 & 0 & 0 & 0 & 0 \\ 0 & 0 & 0.05 & 0.04 & 0.01 & 0 & 0 \\ 0 & 0 & 0 & 0 & 0 & 0.001 & 0.001 \\ 1.0 & 0 & 0 & 0 & 0 & 0 & 0 \\ 1.0 & 0 & 0 & 0 & 0 & 0 & 0 \\ 1.0 & 0 & 0 & 0 & 0 & 0 & 0 \\ 1.0 & 0 & 0 & 0 & 0 & 0 & 0 \end{pmatrix}$$

This set of probabilities is designed to yield in the deterministic limit the values $\phi_f = 0.40$, $\phi_T = 0.50$, $\phi_p = 0.25$, $\tau_B = 10$ itn, and $\tau_C = 500$ itn. Using a $(100 \times 100) = 10\,000$ cell grid, it was found that virtually all (more than 99.9%) of the cells reached the "ground" (A) state before 4000 iterations. Yields for the various pathways could be determined from sums of cells passing through the corresponding virtual states. The "singlet" (B) state lifetime was estimated from linear regression of the natural logarithm of the decay profile for this state. Because the "triplet" (C) state has a finite rise time (see, for example, Figure 3), reflecting its population from the decaying B state, its lifetime was estimated from linear regression of the decay over the interval 100−1000 itn. The values obtained for these properties from trials of 4000 itn are shown in Table 3. They are seen to correspond rather closely to the expected deterministic results.

Steady-State Mode. To simulate this condition, the simple model was first tested with P_{AB} set to several nonzero values that might correspond, for example, to differing levels of exciting light intensity. Keeping the other parameters set as indicated in the transition matrix **P** above, steady-state conditions were reached after a few hundred iterations. At a value $P_{AB} = 0.001$, which corresponds to a moderately strong exciting light intensity, the excited-state populations of the B and C states remain relatively small as the (fluctuating) steady-state condition is achieved. The time-dependent variations in the state populations for $P_{AB} = 0.001$ and $P_{AB} = 0.01$ are shown in Figure 4. It is clear that as P_{AB} increases the steady-state populations of

TABLE 1: Results for 10 Trials with a Single Cell Using the Simple Three-State Model. Times Are Half-Lives in Iterations (itn)

	trial										
	1	2	3	4	5	6	7	8	9	10	average
$\tau_{1/2}$(B)	12	13	51	33	2	1	22	16	5	1	15 ± 16
$\tau_{1/2}$(C)		77		55	30		300	37			100 ± 113
ϕ_f	1	0	1	0	0	1	0	0	1	1	0.50 ± 0.53

TABLE 2: Results for 10 Trials Using the Simple Model with Differing Cell Counts

no. of cells	$\tau_{1/2}$(B)	$\tau_{1/2}$(C)
1	15 ± 16	100 ± 113
10	9.0 ± 4.9	53.1 ± 25.6
100	7.2 ± 1.1	57.4 ± 13.0
1000	6.4 ± 0.4	70.3 ± 4.2
10 000	6.57 ± 0.08	70.1 ± 1.4

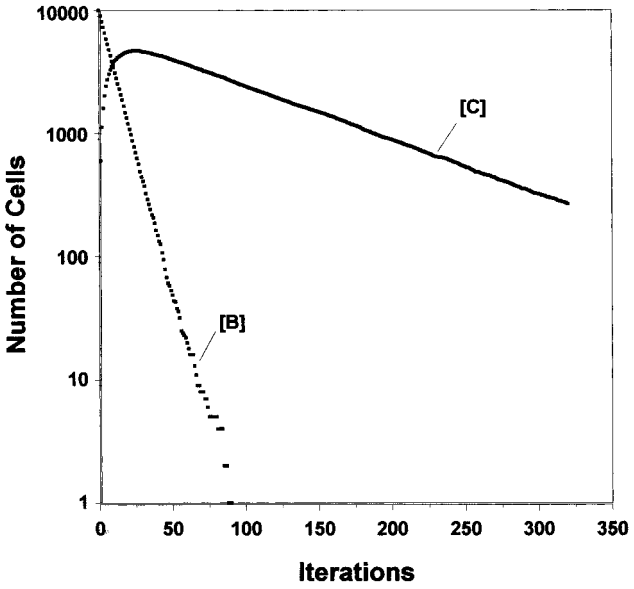

Figure 3. Time variations of the populations of B and C states for a simple 10 000-cell cellular automaton under pulse conditions.

TABLE 3: Results for Various Properties Using the Extended Seven-State Model in Pulse Mode with a (100 × 100) Grid

property	average	range
τ(B)[a]	9.37 ± 0.16	9.18−9.60
τ(C)[a]	492 ± 14	476−510
ϕ_f[b]	0.4007 ± 0.0036	0.3944−0.4057
ϕ_T[b]	0.5002 ± 0.0038	0.4949−0.5052
ϕ_p[b]	0.2505 ± 0.0036	0.2469−0.2579

[a] Five trials. [b] Ten trials.

the excited states B and C increase substantially and the population of the ground state becomes depleted, in accord with the experimental effect observed at high illumination. The effect is especially notable for the "high-intesity illumination" case $P_{AB} = 0.01$, where the surrogate triplet state C obtains a significant steady-state population. Average values (standard deviations in parentheses and ranges in brackets) for the final 100 iterations of 500-iteration trials for these two cases were

	[A]	[B]	[C]
$P_{AB} = 0.001$	9348 (±9)	94 (±8)	558 (±7)
	[9332−9368]	[73−106]	[538−572]
$P_{AB} = 0.01$	5850 (±23)	571 (±24)	3578 (±22)
	[5797−5905]	[514−621]	[3528−3624]

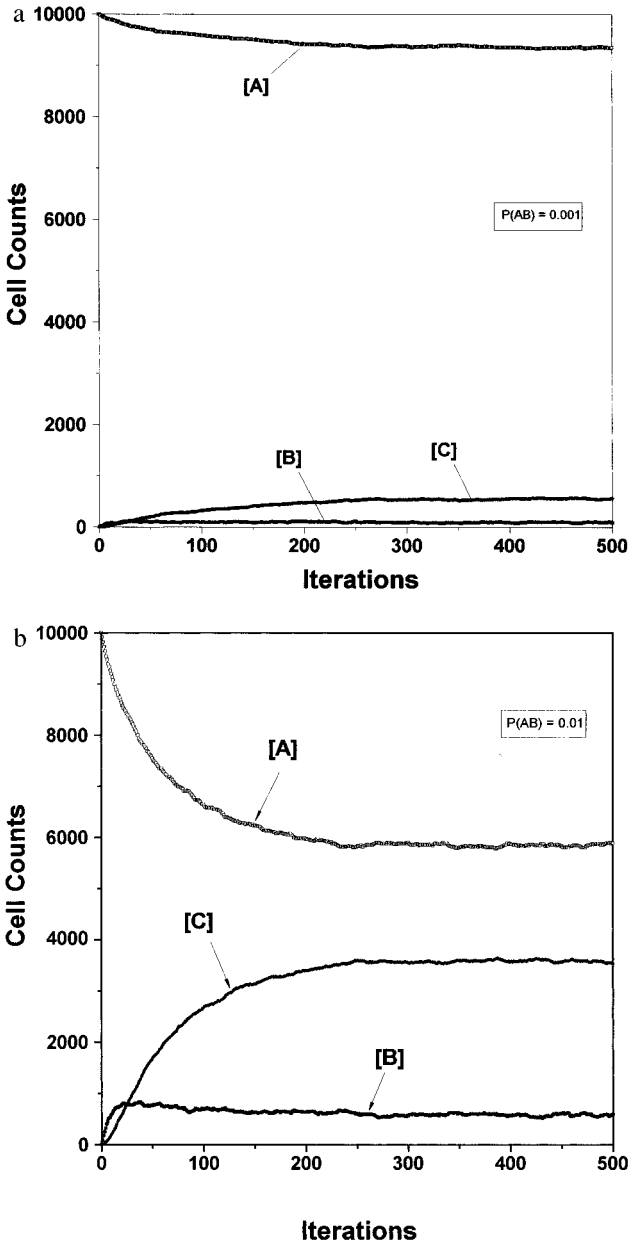

Figure 4. Time variations of the populations of the states of a simple 10 000-cell cellular automaton under steady-state conditions: (a) with $P_{AB} = 0.001$, (b) with $P_{AB} = 0.01$.

The fluctuations are seen to increase substantially for the "high-intensity" case.

Steady-state conditions were next simulated using the extended model of Figure 2b by setting $P_{AB} = 0.001$ in matrix **P′**. The results are shown in Figure 5a for a case where [A] = 10 000 at the start of the trial. Steady-state conditions, with their inherent fluctuations, are reached after about 1500 iterations. (Essentially the same steady-state conditions were also achieved when all cells were in their B states at the start of a run.) Taking the final 1000 itn of the above 5000 itn trial, the following values (standard deviations in parentheses and ranges in brackets) were found:

	[A]	[B]	[C]
$P_{AB} = 0.001$	7919 (±19)	80 (±10)	1994 (±20)
	[7875−7963]	[52−113]	[1956−2041]

Thus under these steady-state conditions roughly 79% of the cells are found in state A, about 1% in state B, and 20% in

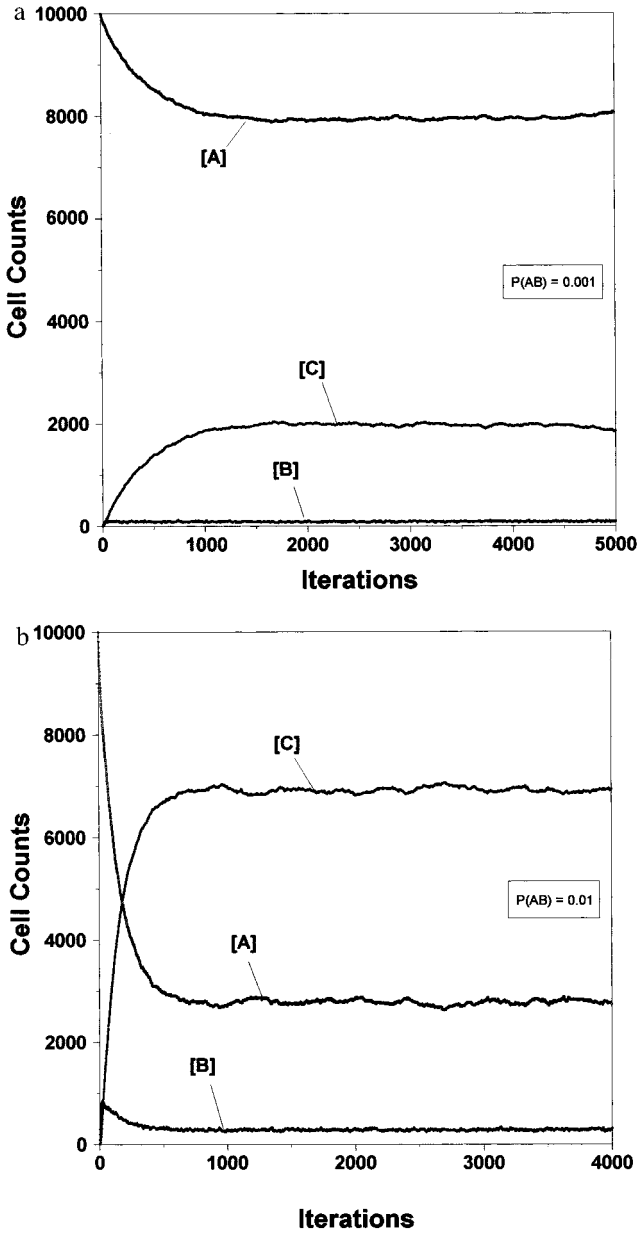

Figure 5. Time variations of the populations of the A, B, and C states of the extended seven-state model for a 10 000-cell cellular automaton under steady-state conditions: (a) with $P_{AB} = 0.001$, (b) with P_{AB} 0.01.

state C. Normally fewer than 0.1% of the cells are in the virtual states at any time after the steady-state condition is reached.

Changing the "triplet" yield by, for example, increasing P_{BC} to 0.08 and decreasing P_{BD} to 0.01 has only a relatively small effect on the steady-state populations. One finds roughly 71% in state A, less than 1% in state B, and 28% in state C under these conditions.

Increasing the excitation probability P_{AB}, however, has a significant effect on the steady-state populations. Setting $P_{AB} = 0.01$ and keeping the other probabilities as shown in matix **P′** yields the curves shown in Figure 5b. It is seen that under these conditions a *population inversion* is achieved, with roughly 69% of the cells in the surrogate triplet state C under steady-state conditions. Now only about 28% of the cells are in the "ground" A state, and the "singlet" B state population is just under 3%, significantly higher than that for the "lower intensity" condition. These results are in contrast to those found earlier for the simple model for which the C-state decay probability was $P_{CA} = 0.01$ and for which no population inversion was achieved. It is apparent that decreasing the C-state decay probability by a factor of 5, or alternatively, increasing the lifetime of this state by the same factor, has had a dramatic effect. Thus the relative state populations are seen to depend crucially on the light intensity, represented here by P_{AB}, and the metastable state lifetime, determined by the total transition probabilities of the pathways depopulating state C.

Conclusions

Two relatively simple cellular automata models of molecular excited-state dynamics have been presented. Both pulse and steady-state modes of behavior can be simulated by the models. The simple three-state model shows the time-dependent variations in state populations in an especially attractive, heuristic way. The extended seven-state model, which employs virtual states, allows competing radiative and nonradiative channels to be distinguished and the corresponding quantum yields of these pathways to be discerned. Thus properties such as the fluorescence and phosphorescence lifetimes and the quantum yields of fluorescence, triplet state formation, and phosphoresence emerge in a natural manner. Both models can be applied to samples as small as a single molecule and demonstrate the stochastic variations to be expected in the state populations and properties for finite samples. Traditional deterministic values for the properties emerge as statistical averages in the limit of large numbers of cells or trials.

It is apparent that suitably constructed cellular automata models accurately reproduce the major features and stochastic variations of molecular excited-state dynamics. In addition, we argue that the cellular automaton models, which simulate aggregate effects from individual events, are in fact more realistic representations of the atomic and molecular level phenomena to which they correspond (and which likewise depend on discrete events) than are the deterministic coupled differential rate equations. Cellular automata models, therefore, should be highly useful for a wide variety of applications involving the simulation and analysis of other molecular dynamic processes.

Acknowledgment. This is the second report under Project ARCH, describing applications of cellular automata to chemical phenomena. The cellular automata simulations were run using the program DING-HAO.

References and Notes

(1) Moerner, W. E.; Kador, L. *Phys. Rev. Lett.* **1989**, *62*, 2535−2538.
(2) Moerner, W. E. *Accts. Chem. Res.* **1996**, *29*, 563−571.
(3) Keller, R. A.; Ambrose, W. P.; Goodwin, P. M.; Jett, J. H.; Martin, J. C.; Wu, M. *Appl. Spectrosc.* **1996**, *50*, 12A−32A.
(4) Goodwin, P. M.; Ambrose, W. P.; Keiler, R. A. *Acc. Chem. Res.* **1996**, *29*, 607−613.
(5) Xie, X. S. *Acc. Chem. Res.* **1996**, *29*, 598−606.
(6) Barnes, M. D.; Whitten, W. B.; Ramsey, J. M. *Anal. Chem.* **1995**, *67*, 418A−423A.
(7) Enderlein, J.; Robbins, D. L.; Ambrose, W. P.; Goodwin, P. M.; Keller, R. A. J. *Phys. Chem. B* **1997**, *101*, 3626−3632.
(8) Lu, H. P.; Xie, X. S. *Nature* **1997**, *385*, 143−146.
(9) Xu, X.-H.; Yeung, E. S. *Science* **1997**, *275*, 1106−1109.
(10) Seybold, P. G.; Kier, L. B.; Cheng, C.-K. *J. Chem. Inf. Comput. Sci.* **1997**, *37*, 386−391.
(11) Magde, D. In *Kirk-Othmer Encyclopedia of Chemical Technology*; John Wiley & Sons: New York, 1995; Vol. 14, pp 1021−1044.
(12) Seybold, P. G.; Gouterman, M. *Chem. Rev.* **1965**, *65*, 413−433.
(13) Avouris, P.; Gelbart, W.; El-Sayed, M. L. *Chem. Rev.* **1977**, *77*, 793−833.
(14) Parker, C. A. *Photoluminescence of Solutions*; Elsevier Publ. Co.: New York, 1968.
(15) Birks, J. B. *Photophysics of Aromatic Molecules*; Wiley-Interscience: New York, 1970.

(16) Lakowicz, J. R. *Principles of Fluorescence Spectroscopy*; Plenum Press: New York, 1983.
(17) Kasha, M. *Discuss. Faraday Soc.* **1950**, 9, 14−19.
(18) Ulam, S. M. *Proc. Int. Congr. Math.* (held in 1950) **1952**, *2*, 262.
(19) von Neumann, J. *Theory of Self-Reproducing Automata;* Univ. of Illinois Press: Urbana, 1966.
(20) d'Humières, D. In *Cellular Automata and Modeling of Complex Physical Systems*; Manneville, P., Boccara, N., Vichniac, G. Y., Bidaux, R., Eds.; Springer-Verlag: Heidelberg, 1990; pp 186−204.
(21) Cornell, S.; Droz, M.; Chopard, B. *Physica A* **1992**, *188*, 322−336.
(22) Chopard, B.; Luthi, P.; Droz, M. *Phys. Rev. Lett.* **1994**, *72*, 1384−1387.
(23) Lawniczak, A.; Dab, D.; Kapral, R.; Boon, J.-P. *Physica D* **1991**, *47*, 132−158.
(24) Dab, D.; Boon, J.-P.; Li, Y.-X. *Phys. Rev. Lett.* **1991**, *66*, 2535−2538.
(25) Gerhardt, M.; Schuster, H.; Tyson, J. J. *Science* **1990**, *247*, 1563−1566.
(26) Ermentrout, G. B.; Edelstein-Keshet, L. J. *Theoret. Biol.* **1993**, *160*, 97−133.
(27) Levin, S. A.; Grenfell, B.; Hastings, A.; Perelson, A. S. *Science* **1997**, *275*, 334−343.
(28) Hayes, B. *Am. Sci.* **l994**, *82*, 206−210.
(29) Epstein, J. M.; Axtell, R. *Growing Artificial Societies: Social Science from the Bottom Up*; Brookings Inst./MIT Press: Washington, DC, 1996.
(30) Markus, M.; Hess, B. *Nature* **1990**, *347*, 56−58.
(31) Kapral, R.; Showalter, K., Eds. *Chemical Waves and Pattems*; Kluwer Acad. Publ.: Boston, 1995.
(32) Vanag, V. K. J. *Phys. Chem.* **1996**, *100*, 11336−11345.
(33) Kier, L. B.; Cheng, C.-K. J. *Chem. Inf. Comput. Sci.* **1994**, *34*, 647−652.
(34) Kier, L. B.; Cheng, C.-K. *Pharm. Res.* **1995**, *12*, 1521−1525.
(35) Kier, L. B.; Cheng, C.-K.; Testa, B.; Carrupt, P.-A. *Pharm. Res.* **1995**, *12*, 615−620.
(36) Kier, L. B.; Cheng, C.-K. *J. Math. Chem.* **1997**, *21*, 71−81.
(37) Kier, L. B.; Cheng, C.-K. In *Lipophilicity in Drug Action and Toxicology*; Pliska, V., Testa, B., van de Waterbeemd, H., Eds.; VCH Publishers: New York, 1996; pp 181−194.
(38) Kier, L. B.; Cheng, C.-K.; Testa, B.; Carrupt, P.-A. *Pharm. Res.* **1996**, *13*, 1419−1422.
(39) Kier, L. B.; Cheng, C.-K.; Testa, B.; Carrupt, P.-A. J. *Pharm. Sci.* **1997**, *86*, 774−778.
(40) Kier, L. B.; Cheng, C.-K.; Testa, B.; Carrupt, P.-A. J. *Mol. Graphics* **1996**, *14*, 227−231.
(41) Kier, L. B.; Cheng, C.-K. *J. Theoret. Biol.* **1997**, *186*, 75−80.
(42) *StatMost*; DataMost Corporation: P.O. Box 65389, Salt Lake City, UT 65389, 1995.